



Role of gas fragmentation in the formation of supermassive black hole seeds

M. Suazo¹, J. Prieto¹ & A. Escala¹

¹ *Departamento de Astronomía, Universidad de Chile, Santiago, Chile.*

Contact / matias.suazo@ug.uchile.cl

Resumen / Observaciones de cuásares en etapas tempranas del universo muestran que estas estructuras ya albergaban agujeros negros supermasivos de hasta $10^9 M_{\odot}$. Radiación de fondo UV parece ser clave en la formación de semillas masivas de agujeros negros, ya que su presencia calienta el ambiente, y suprime refrigerantes moleculares permitiendo la formación de una estructura masiva. En este trabajo presentamos simulaciones cosmológicas realizadas con el código hidrodinámico RAMSES con el fin de estudiar la formación de semillas en diferentes escenarios. Nuestros resultados muestran que la radiación UV no es un único factor determinista en la formación de semillas masivas, la dinámica también parece ser importante. Esto, porque la dinámica es capaz de cambiar las condiciones de formación de semillas.

Abstract / High redshift quasars observations show that they already hosted supermassive black holes with masses up to $10^9 M_{\odot}$. The UV background intensity seems to be a key parameter in the formation of massive seeds, since its presence heats the environment and suppresses molecular coolants, allowing the formation of a massive structure. Several cosmological simulations performed with the hydrodynamical code RAMSES are presented in this work to study the formation of seeds in different scenarios. Our results show that UV radiation does not determine the feasibility of forming massive seeds as a unique parameter, since other factors like gas dynamics may alter the formation of such objects.

Keywords / methods: numerical — quasars: supermassive black holes

1. Introduction

Quasars are intriguing astrophysical objects. They are primordial galaxies powered by supermassive black holes (SMBHs) in their centers. Observations of $z > 6$ quasars (Bañados et al., 2018) show that these objects already hosted SMBHs with masses up to $10^9 M_{\odot}$ when the universe was ~ 0.7 Gyr old. The formation of such massive objects is still a puzzle. Various mechanisms to form these structures have been proposed. For further reading, see Volonteri (2010) and Latif & Ferrara (2016).

Of all scenarios, direct collapse black hole (DCBH) model has been shown to be efficient in forming massive seeds. It consists of the immediate collapse of a gas cloud into a seed of $10^4 - 10^6 M_{\odot}$. In this model, the seed would ultimately collapse into a black hole keeping most of its mass. The seeds need to accrete at rates $\geq 0.1 M_{\odot} \text{ yr}^{-1}$ (Schleicher et al., 2013; Sakurai et al., 2015). However, this scenario demands strict conditions. A very massive halo is indeed necessary to have the gas reservoir to form a massive seed and also to ensure high gas temperature (~ 8000 K) to allow atomic cooling to operate. An intense UV background is also required in order to dissociate molecular hydrogen: an efficient coolant in this epoch. This radiation has been typically justified by setting a star forming galaxy in the surrounding of the possible DCBH. In comparison to molecular and metal cooling, atomic cooling is characterized by acting more smoothly in the temperature ranges involving DCBH conditions, permitting

an isothermal collapse that does not produce fragments (Latif et al., 2013b, 2014).

Though the DCBH model may explain the formation of massive seeds, there are still some obstacles that gas needs to overcome. One obstacle arises when gas is photo-evaporated, in which case a dense core is prevented to be formed. Ionization also impedes the formation of a central structure, since it leads to an increase in the electron fraction, which is one of H_2 catalysts (Johnson et al., 2014). Another obstacle corresponds to the tidal interaction that the neighborhood may be exerting against the pristine halo, that could disrupt it, avoiding the formation of a massive central object (Chon et al., 2016).

The purpose of this work is to study the feasibility of forming massive black hole seeds in halos where fragmentation is allowed.

2. Methodology

We performed a set of three simulations in box sizes of $1 h^{-1} \text{ Mpc}$ in comoving units using the adaptive mesh refinement hydrodynamical cosmological code RAMSES (Teyssier, 2002). Initial conditions were created using the MUSIC code (Hahn & Abel, 2011). We got a maximum resolution of 10^{-2} pc in proper units. The cosmology used is the one given by the Planck Collaboration et al. (2016) that sets $\Omega_b = 0.3089$, $\Omega_{\Lambda} = 0.6911$, $\sigma_8 = 0.8159$, $n_s = 0.9967$, $H_0 = 67.74 \text{ km s}^{-1} \text{ Mpc}^{-1}$. We used 32 cells per Jeans length as the minimum rea-

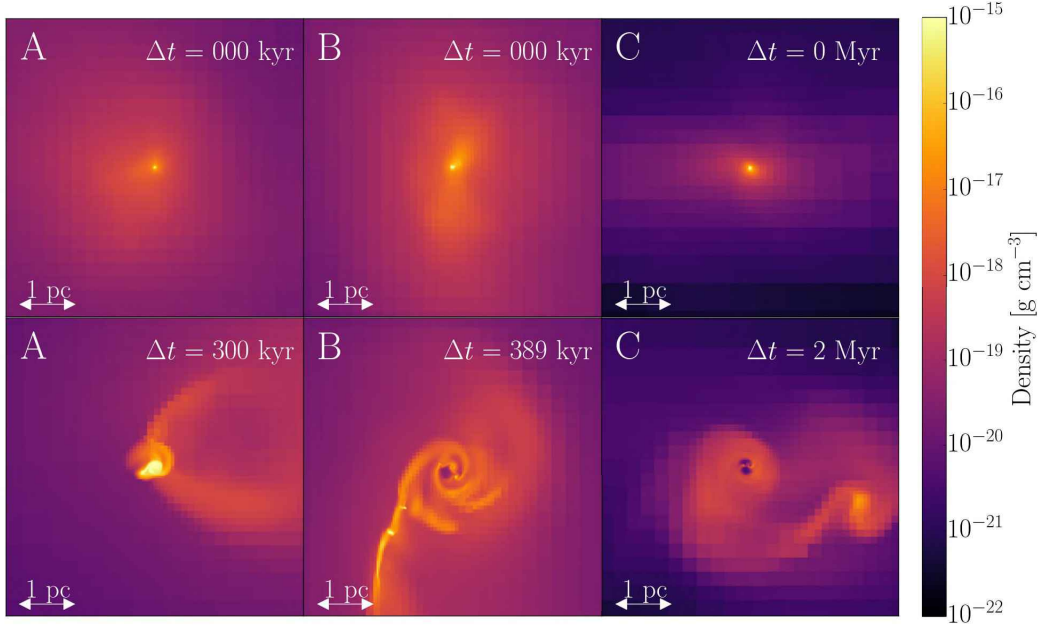


Figure 1: Density projection for all re-simulated halos irradiated by a uniform UV background. Halos A and B are under the effect of $J_{21} = 10000$, while C is irradiated by a UV background of $J_{21} = 10$. In all cases 5 pc are projected, and Δt is the time relative at which the first sink particle is formed in the re-run respectively.

sonable value suggested by Latif et al. (2013a) to resolve turbulences. No scheme for radiative transfer is included.

2.1. Chemical model

The thermal and chemical evolution of the gas were solved employing the publicly available package KROME (Grassi et al., 2014). We used a primordial chemistry network made up of the following species: H, H^+ , H^- , He, He^+ , He^{++} , e^- , H_2 , H_2^+ . We assumed a uniform isotropic UV background of various intensities that would come from a star forming neighborhood. The spectra of those regions are black-bodies with $T_{\text{eff}} = 2 \times 10^4$ K, which is in the range that mimics realistic spectra (Latif et al., 2015).

2.2. Sink particles

The gravitational collapse of dense regions is a phenomenon quite recurrent in astrophysical simulations, therefore, a huge dynamical range is required. However, computational resources are not always sufficient to resolve the small scales. As a consequence, some numerical artifacts have arisen, one of them being the so-called sink particles.

Sink particles are particles that approximate the scales that are not resolved by the collapse of a region into a single point. A modified algorithm to the one presented in the RAMSES code (Bleuler & Teyssier, 2014) was used to create sink particles. It considers: the cell

Table 1: Virial mass, spin parameter and number of particles in the low resolution DM-only simulated halos.

Halo	Virial Mass [M_{\odot}]	Spin parameter	n_{part}
A	9.68×10^7	0.016	1612
B	2.68×10^8	0.038	4471
C	4.90×10^7	0.022	821

from which the sink particle will form has to be in the highest level of refinement, also the mass of such cell has to be larger than its Jeans mass.

3. Results

We performed 3D simulations to study the effect of gas fragmentation in the formation of primordial SMBH seeds in three different halos. We started from only Dark Matter (DM) low resolution simulations initialized at $z = 99$ in 1 comoving h^{-1} cMpc box sizes, in order to re-simulate some of them. Halo masses were required to be higher than $\sim 5 \times 10^7 M_{\odot}$ to guarantee the virial temperature to be in the atomic cooling regime (> 8000 K), in which gas is mainly cooled down due to electronic transitions in the hydrogen atom. We identified dark matter halos using the HOP clump finder (Eisenstein & Hut, 1998).

Three halos were selected to be re-simulated, some of their properties are shown in Table 1, which includes virial mass, bullock spin parameter (Bullock et al., 2001), and number of particles. Halos A and B were

re-simulated including a strong uniform UV background with a $J_{21} = 10000$ value, while halo C was re-simulated including a weak uniform UV background with a $J_{21} = 10$ value. J_{21} stands for $10^{-21} \text{ erg s}^{-1} \text{ Hz}^{-1} \text{ cm}^{-2} \text{ str}^{-1}$.

In Fig. 1 we show density projections for our re-simulated halos under the presence of a uniform UV background according to the values mentioned in the paragraph above. In all these cases 5 pc are projected, and Δt refers to the time relative at which the first sink particle is formed in each run respectively. The first sink particle in halo A is formed at $z = 11.28$ (400.1 Myr), in halo B it is formed at $z = 10.80$ (425 Myr), and in halo C it is at $z = 11.03$ (412.5 Myr).

Halo A is shown in the leftmost column, B is represented in the middle column, and C is pictured in the rightmost column. Top row represents the state of the central 5 pc at the time the first sink particle is formed in each simulation, while the bottom row represents an evolved stage of the same region. Δt values chosen in this row were based on portraying changes in the structure, also to reveal the differences in the timescales to see them. In halos A and B projections are performed along the axis at which the structure is perpendicular. In halo C several structures are formed, so the projection was made along the z -axis arbitrarily. Projections are centered in the position of the first sink particle created.

Halo A initially starts as a central, dense spherical structure with a single sink particle in its center (not shown). As the simulation advances, the central structure acquires some asymmetries, but they do not affect its growing, fragmentation is not seen either. Just one sink particle is formed and it reaches $8.8 \times 10^4 M_{\odot}$ at the end of the run. On the other hand, halo B behaves in a different way, it begins as a central dense object with a single sink particle in the center in the similar fashion to A, however it soon fragments forming a spiral-like structure as time goes on, from which new sink particles are formed. After a sink particle merging episode, the most massive sink particle ends up with $5.5 \times 10^4 M_{\odot}$. In both halos 5 pc represent the extent of all structures formed. Finally, in halo C there is a similar behavior to the other cases: a central, dense structure is observed, and evolves into a spiral-like structure from which new sink particles are created. However, in Fig. 2 we can see a 100 pc region encompassing all features in this halo at the end of the run. Unlike the others, fragmentation happens at a larger scale, forming various cored regions. The most massive sink particles ends up with $1.6 \times 10^4 M_{\odot}$ at the end of the run after three merger episodes.

4. Conclusion

We got very different outcomes for our variety of halos. Halo A can be seen as the *traditional* DCBH scenario, since it forms a very dense, central object, whose central sink particle reaches a mass close to $10^5 M_{\odot}$. Halo B is very similar to the DCBH in terms of the timescale and the final mass observed, however, it is the outcome of fragmentation and merger episodes. Simulations A and B have in common the same intensity value in the UV background. Despite of this, we find that the UV

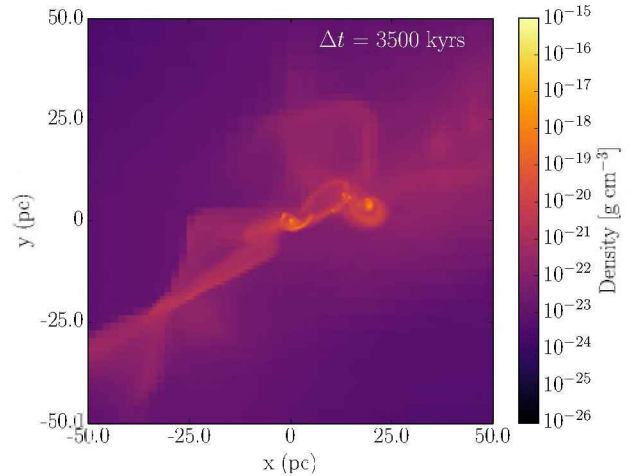


Figure 2: Density projection at 100 pc for halo C at the end of this run.

background is not the only parameter determining the behavior of the structure formed, since the history of the dark matter halo is different for everyone and matters. In halo C fragmentation also occurs, but unlike halo B, the scales where this process happen are larger, observed from 5 pc up to 100 pc. Unlike halos A and B, timescales for halo C are larger for one order of magnitude. Though the most massive sink particle in halo C is the lightest compared to the other halos, it is still very massive, and it can still grow through new merger episodes.

Acknowledgements: We received partial support from Center of Excellence in Astrophysics and Associated Technologies (PFB 06). We acknowledge partial support from FONDECYT through grant 1181663. The Geryon cluster at the Centro de Astro-Ingenieria UC was extensively used for the calculations performed in this work. BASAL CATA PFB-06, the Anillo ACT-86, FONDEQUIP AIC-57, and QUIMAL 130008 provided funding for several improvements to the Geryon cluster. Powered@NLHPC: This research was partially supported by the supercomputing infrastructure of the NLHPC (ECM-02).

References

- Bañados E., et al., 2018, *Nature*, 553, 473
- Bleuler A., Teyssier R., 2014, *MNRAS*, 445, 4015
- Bullock J.S., et al., 2001, *ApJ*, 555, 240
- Chon S., et al., 2016, *ApJ*, 832, 134
- Eisenstein D.J., Hut P., 1998, *ApJ*, 498, 137
- Grassi T., et al., 2014, *MNRAS*, 439, 2386
- Hahn O., Abel T., 2011, *MNRAS*, 415, 2101
- Johnson J.L., et al., 2014, *MNRAS*, 445, 686
- Latif M.A., Ferrara A., 2016, *PASA*, 33, e051
- Latif M.A., et al., 2013a, *MNRAS*, 430, 588
- Latif M.A., et al., 2013b, *MNRAS*, 436, 2989
- Latif M.A., et al., 2014, *ApJ*, 792, 78
- Latif M.A., et al., 2015, *MNRAS*, 446, 3163
- Planck Collaboration, et al., 2016, *A&A*, 594, A13
- Sakurai Y., et al., 2015, *MNRAS*, 452, 755
- Schleicher D.R.G., et al., 2013, *A&A*, 558, A59
- Teyssier R., 2002, *A&A*, 385, 337
- Volonteri M., 2010, *A&A Rv*, 18, 279